


Article

Multi-Ship Collision Avoidance Decision-Making Based on Collision Risk Index

Yingjun Hu ¹, Anmin Zhang ^{1,2,*}, Wuliu Tian ^{3,*}, Jinfen Zhang ⁴ and Zebei Hou ¹

¹ School of Marine Science and Technology, Tianjin University, Tianjin 300072, China; lucky9_hyj@sina.com (Y.H.); discover4hj@163.com (Z.H.)

² Tianjin Port Environmental Monitoring Engineering Center, Tianjin 300072, China

³ Maritime College, Beibu Gulf University, Qinzhou 535011, China

⁴ National Engineering Research Center for Water Transport Safety, Wuhan University of Technology, Wuhan 430070, China; jinfen.zhang@whut.edu.cn

* Correspondence: zhanganmin@sina.com (A.Z.); tianwuliu@foxmail.com (W.T.)

Received: 26 July 2020; Accepted: 18 August 2020; Published: 20 August 2020



Abstract: Most maritime accidents are caused by human errors or failures. Providing early warning and decision support to the officer on watch (OOW) is one of the primary issues to reduce such errors and failures. In this paper, a quantitative real-time multi-ship collision risk analysis and collision avoidance decision-making model is proposed. Firstly, a multi-ship real-time collision risk analysis system was established under the overall requirements of the International Code for Collision Avoidance at Sea (COLREGs) and good seamanship, based on five collision risk influencing factors. Then, the fuzzy logic method is used to calculate the collision risk and analyze these elements in real time. Finally, decisions on changing course or changing speed are made to avoid collision. The results of collision avoidance decisions made at different collision risk thresholds are compared in a series of simulations. The results reflect that the multi-ship collision avoidance decision problem can be well-resolved using the proposed multi-ship collision risk evaluation method. In particular, the model can also make correct decisions when the collision risk thresholds of ships in the same scenario are different. The model can provide a good collision risk warning and decision support for the OOW in real-time mode.

Keywords: maritime transportation; collision risk index; collision avoidance decision-making; COLREGs

1. Introduction

Shipping has been one of the dominant modes of global trade, which accounts for more than 90% of international cargo trade [1]. Ship collision is a major type of maritime accident that often results in significant casualties, environmental pollution and economic losses. Even though ships have many advanced equipment (e.g., Automatic Identification System, AIS, Automatic Radar Plotting Aids, ARPA and Integrated Navigation Systems, INS), it is stated that, in many marine accident surveys, more than 80% of maritime traffic accidents are related to human factors [2–5]. Therefore, the impact of human factors on accidents still plays an important role [6–8]. It is therefore complex and important to focus on the decision-making process of ship collision avoidance. Particular attention is paid to the fact that the maneuvering difficulty of the officer on watch (OOW) increases exponentially in harbors and sea areas with much higher density ship traffic flows. The International Maritime Organization (IMO) issued International Code for Collision Avoidance at Sea (COLREGs) in 1972 [9]. The COLREGs outline ship-related navigation rules and concepts, which requires all ships engaged in international voyages to comply with the convention. Therefore, Hilgert, H et al. [10] have been

profoundly and comprehensively discussed. In practice, OOWs still have many subjective decisions by virtue of subjective experience under the limited constraints of the rules. That is to say, the OOWs are highly subjective in the collision-avoidance process. Moreover, different OOWs may have substantial differences in measuring the collision risk, especially when more than two ships meet each other and there is collision risk among them (multi-ship encounter situations). This would influence their subsequent decision-makings, and conflicts among the encountered ships would occur. There is a wide range in measuring risk by OOWs.

Ship collision risk modeling and risk analysis studies have become major research interests in recent decades [11–13], which are the basis and precondition for collision-avoidance decisions. The collision risk index (CRI) is used to assess the probability and severity of a ship collision with other ships in the vicinity. Many accidents are caused by a reluctant or no reaction [14,15]. Therefore, it is significant to provide the OOWs with objective and valid data for a collision risk analysis.

A ship collision risk assessment has multiple approaches. The concept of a ship domain was introduced by Fujii in 1971 [16], which allows a simple assessment of the risk of ship collisions. Later on, the ship domain model was further improved by Goodwin and Coldwell [17,18]. Especially in the last decades, many researchers have introduced various sizes and shapes of ship domain models [19–21]. However, none of the ship domain models addressed the time dimension of the ship motion information. Baldauf, M et al. [22] proposed a “last line of defense” that has been defined for collision avoidance based on calculations and the prevailing environmental conditions, which greatly reduced the number of collisions at sea. There are several models for evaluating ship collision risks, such as the ship domain model, the fuzzy logic model and the minimum distance to collision (MDTC) model that considers maneuverability [11,23,24]. With the introduction of COLREGs and the development of ship collision risk models, intelligent optimization methods have been investigated to achieve real-time and reliable ship collision avoidance [25], such as neural networks [26], fuzzy mathematics [27] and reinforcement learning [28]. Meanwhile, fuzzy mathematics can also be applied to fuzzy collision risk classification and fuzzy inference [29–31]. The performance of fuzzy mathematics depends on a preset membership function, which requires more a priori knowledge [32,33]. The idea of fuzzy logic is widely used to deal with the dynamic and static parameters of ship navigation (e.g., ship position, speed, heading, etc.) obtained by aids to navigation instruments, which the main factors influencing the collision risk of a ship were created to evaluate the set of collision risk [32–36].

Ship collision avoidance decision-making is another focus of many researchers, and the major ship collision avoidance decision-making algorithms can be divided into two categories, which are heuristic algorithms and deterministic algorithms. Heuristic algorithms mainly include the A* algorithm, artificial potential field (APF), neural networks and other intelligent optimization algorithms. The A-star (A*) algorithm is a global heuristic search algorithm that mainly considers the start and end positions and is able to obtain the planned path. Chen et al. [37] and Wang et al. [38] proposed a path search through a hierarchical planning approach that can ultimately yield relatively more efficient paths. The path-planning method for ships in wind farm waters based on the multi-directional A* algorithm was proposed by Xie et al. [39]. Liu et al. [40] used the A* algorithm to take the chart water depth as one of the constraints for path planning and performed a path search and hydrodynamic analysis. They achieve the goals of path planning and collision avoidance decision-making through an improved A* algorithm. However, APF is different from the A* algorithm; the paths generated by the APF method are smoother than those of the A* method and more closely match the navigation reality. Therefore, the APF algorithm has also been well-used in recent years. Besides, the intelligent optimization algorithm is a class of probability-based stochastic search evolutionary algorithms, which deals with the problem of intelligent route planning and multi-objective collision avoidance decisions.

Besides heuristics algorithms, deterministic algorithms also have attracted the attention of many researchers, including steering timing and steering magnitude decisions, multiple intelligences methods and logic coding. In maritime practice, ship collision avoidance decision-making algorithms should make decisions that are as easy for the OOW to operate as possible. Zhang et al. [41] proposed a linear

extension algorithm to study the multi-ship collision avoidance decision problem, which has been shown to be an effective method. The results obtained can be closely aligned with sailing practices, focusing on the analysis of the number and magnitude of turns, as well as the time spent sailing on the new course during the decision-making process. Kim et al. [42] used the distributed local search algorithm (DLSA) and the distributed taboo search algorithm (DTSA) to find the best heading for the ship in question. Ships would reduce the risk of collision by changing course. In addition, Kim et al. [43] presented a distributed random search algorithm. The algorithm allows each ship to change its intentions in a random manner as soon as it receives all intentions from the target ship (TS), which is planned by changing the course. Similarly, Li et al. [44] proposed a new method for collision avoidance in the case of multi-ship encounters. With the rapid development of deep learning, many researchers have started to use deep reinforcement learning (DRL) methods to solve the problem of collision avoidance decision-making [45–47]. DRL is able to have good adaptability in complex environments. Ozoga et al. [48] proposed a multi-objective ARPA system that provided the OOWS with a few of the operational information about navigational safety when the ship encounters other ships. These deterministic algorithms are based on a multi-vessel perspective and plan the voyage path in a collaborative manner to prevent collisions. In summary, both heuristics and deterministic algorithms have been studied to avoid collisions.

A real-time collision risk analysis and multi-ship collision avoidance decision support model are studied in this paper. In this model, we mainly consider the actual operational habits of the OOW to provide objective support. At the same time, we also consider COLREGs, collision risk assessment and collision avoidance decision from the ship's own perspective. Besides, the fuzzy logic approach is applied to establishing a ship collision risk quantification and analysis model. The real-time *CRI* can be calculated accordingly as the basis of the ship's collision risk assessment and intelligent collision avoidance, providing the OOW with good auxiliary decision-making and an early warning function. The deterministic collision avoidance decision-making procedure is applied to carry out collision avoidance simulation, and finally, simulations are performed under different reference thresholds of the *CRI*. In particular, the simulations in the case that different *CRI* thresholds for different ships in the same scenario validate the effectiveness of the multi-ship collision avoidance model.

The remainder of the paper is organized as follows: The fundamentals of collision risk assessment are presented in Section 2, mainly including the requirements related to the collision risk index model and COLREGs. In Section 3, the basic concepts of the collision avoidance procedure and the general framework of the collision avoidance decision procedure are presented. The collision avoidance procedure is discussed in Section 4. Section 5 performs several typical multi-ship collision avoidance simulations, along with the discussions on the results. Section 6 concludes the paper.

2. Preliminaries

2.1. Collision Risk Model

In multi-ship encounters, the real-time *CRI* with respect to two ships can be evaluated by the relative motion parameters between the ships [21,49,50], i.e., distance to the closest point of approach (*DCPA*), time to the closest point of approach (*TCPA*), the relative distance (*D*), relative bearing (α_{OT}) and the relative speed (V_{OT}), as shown in Figure 1.

Based on the distribution and for ease of expression, each ship treats itself as the "Own Ship (OS)" from a first-person perspective. The other ships are considered to be "Target Ship (TS)" if it causes an obstacle to the normal navigation of the OS. In a typical encounter, the collision risk index can usually be calculated using relative motion parameters for two ships [33], as shown in Figure 1.

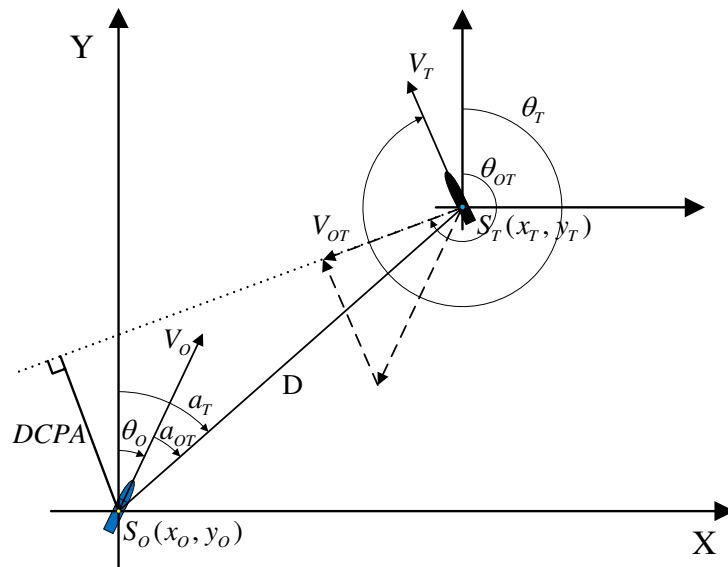


Figure 1. Motion parameters of two ships in a typical encounter situation.

The relative motion parameters are calculated as follows [45]:

$$DCPA = D \times \sin(\theta_{OT} - \alpha_T - \pi) \tag{1}$$

$$TCPA = \frac{D \times \cos(\theta_{OT} - \alpha_T - \pi)}{V_{OT}} \tag{2}$$

$$D = \sqrt{(x_T - x_O)^2 + (y_T - y_O)^2} \tag{3}$$

$$\alpha_{OT} = \alpha_T - \theta_O \pm 2\pi \tag{4}$$

where S_O is the position of OS, S_T is the position of TS, θ_{OT} is the relative course of TS, D is the relative distance to TS, α_T is the true relative position direction to TS, α_{OT} is the angle converted from in the body-fixed coordinate system and V_{OT} is the relative speed of TS.

The intermediate parameters in (1)–(4) can be calculated by:

$$\begin{cases} V_O^x = V_O \sin(\theta_O) \\ V_O^y = V_O \cos(\theta_O) \\ V_T^x = V_T \sin(\theta_T) \\ V_T^y = V_T \cos(\theta_T) \end{cases} \tag{5}$$

$$\begin{cases} V^x = V_T^x - V_O^x \\ V^y = V_T^y - V_O^y \end{cases} \tag{6}$$

$$\begin{cases} x_{OT} = x_T - x_O \\ y_{OT} = y_T - y_O \end{cases} \tag{7}$$

where $X_O = [x_O, y_O, V_O, \theta_O]^T$ is the motion state of the OS, and $X_T = [x_T, y_T, V_T, \theta_T]^T$ is the motion state of TS. V^x and V^y are the relative speed components of the TS on the X and Y axes, respectively, and x_{OT}

and y_{OT} are the relative distance components of the TS on the X and Y axes, respectively. The relative speed of the TS is calculated as follows:

$$\begin{aligned}
 V_{OT} &= \sqrt{(V_{OT}^x)^2 + (V_{OT}^y)^2} \\
 &= \sqrt{(V_O^x - V_T^x)^2 + (V_O^y - V_T^y)^2} \\
 &= V_O \times \sqrt{1 + \left(\frac{V_T}{V_O}\right)^2 - 2 \times \frac{V_T}{V_O} \times \cos(\theta_O - \theta_T)}
 \end{aligned}
 \tag{8}$$

where θ_O is the heading of OS (deg), V_O is the speed of OS (kn), θ_T is the heading of TS (deg) and V_T is the speed of TS (kn). The relative course and the true course of the TS are calculated as follows [45]:

$$\theta_{OT} = \begin{cases} \arctan \frac{V^x}{V^y} & V^x \geq 0 \cap V^y \geq 0 \\ \arctan \frac{V^x}{V^y} + \pi & V^x < 0 \cap V^y < 0 \\ \arctan \frac{V^x}{V^y} + \pi & V^x \geq 0 \cap V^y < 0 \\ \arctan \frac{V^x}{V^y} + 2\pi & V^x < 0 \cap V^y \geq 0 \end{cases}
 \tag{9}$$

$$a_T = \begin{cases} \arctan \frac{x_{OT}}{y_{OT}} & x_{OT} \geq 0 \cap y_{OT} \geq 0 \\ \arctan \frac{x_{OT}}{y_{OT}} + \pi & x_{OT} < 0 \cap y_{OT} < 0 \\ \arctan \frac{x_{OT}}{y_{OT}} + \pi & x_{OT} \geq 0 \cap y_{OT} < 0 \\ \arctan \frac{x_{OT}}{y_{OT}} + 2\pi & x_{OT} < 0 \cap y_{OT} \geq 0 \end{cases}
 \tag{10}$$

Fuzzy logic is good at expressing the knowledge and experience with unclear boundaries, which is similar with the case of the ship collision risk evaluation. Therefore, fuzzy synthesis judgment is introduced [51,52]. For instance, numerous studies have been done by many researchers using fuzzy logic methods to model the level of collision risk through the membership functions [32,33,53]. In view of the fuzziness and uncertainty of the CRI, many researchers have applied the fuzzy comprehensive evaluation method to the evaluation of the CRI. One of the most important aspects of the fuzzy method is to establish the membership functions of the fuzzy set. In practice, in addition to the TCPA and DCPA, other parameters such as the relative distance, relative bearing and speed ratio also have impact on the OOW to evaluate the level of collision risk. In this study, based on the geometry of ship collision, the above parameters are selected as the influencing factors of the CRI calculation, of which the memberships are defined as follows:

(1) The membership function of DCPA [45]:

$$u(DCPA) = \begin{cases} 0 & d_2 < |DCPA| \\ \frac{1}{2} - \frac{1}{2} \sin \left[\frac{\pi}{d_2 - d_1} \left(|DCPA| - \frac{d_1 + d_2}{2} \right) \right] & d_1 < |DCPA| \leq d_2 \\ 1 & |DCPA| \leq d_1 \end{cases}
 \tag{11}$$

In which the process of d_1 and d_2 are shown as follows [45]:

$$d_1 = \begin{cases} 1.1 - \frac{0.2 \times a_{OT}}{\pi} & 0^\circ \leq a_{OT} < 112.5^\circ \\ 1.0 - \frac{0.4 \times a_{OT}}{\pi} & 112.5^\circ \leq a_{OT} < 180^\circ \\ 1.0 - \frac{0.4 \times (2\pi - a_{OT})}{\pi} & 180^\circ \leq a_{OT} < 247.5^\circ \\ 1.1 - \frac{0.2 \times (2\pi - a_{OT})}{\pi} & 247.5^\circ \leq a_{OT} \leq 360^\circ \end{cases}
 \tag{12}$$

$$d_2 = K \times d_1
 \tag{13}$$

where d_1 represents the minimum distance of the two ships, and d_2 represents the safe encounter range. K is the coefficient determined by the factors as the instability of the ship state and the two ships' incoordination and is generally 1.5–2.0 [32]; K is set to 2.0 in this paper. The OOWs can make adjustments on the value according to the navigation environment in practice.

(2) The membership function of $TCPA$ [45]:

$$u(TCPA) = \begin{cases} 0, & t_2 < |TCPA| \\ \left(\frac{t_2 - |TCPA|}{t_2 - t_1}\right)^2, & t_1 < |TCPA| \leq t_2 \\ 1, & 0 \leq |TCPA| \leq t_1 \end{cases} \quad (14)$$

where t_1 is the time of ship collision, which represents the time taken by the giving-way ship from the latest moment of avoidance action to the closest point of approach. t_2 is the time of taking attention to the TS, which represents the time when the ship starts to pay attention to the TS. It is generally accepted that 6–8 nautical miles is the distance at which ships can navigate freely [32]. Therefore, for safety reasons, 8 nautical miles is used in this paper as the distance between ships. Then, we set the time corresponding to t_2 when the closest point of approach from the OS to the TS is no larger than 8 nautical miles. V_{OT} is the relative speed between the two ships. D_1 and D_2 represent the latest operation distance and the safe distance for the give-way ship to take collision avoidance measures. t_1 and t_2 are calculated as follows [45]:

$$t_1 = \begin{cases} \frac{\sqrt{D_1^2 - DCPA^2}}{V_{OT}} & DCPA \leq D_1 \\ \frac{(D_1 - DCPA)}{V_{OT}} & DCPA > D_1 \end{cases} \quad (15)$$

$$t_2 = \begin{cases} \frac{\sqrt{D_2^2 - DCPA^2}}{V_{OT}} & DCPA \leq D_2 \\ \frac{(D_2 - DCPA)}{V_{OT}} & DCPA > D_2 \end{cases}$$

(3) The membership of D [32]:

$$u(D) = \begin{cases} 0, & D_2 < D \\ \left(\frac{D_2 - D}{D_2 - D_1}\right)^2 & D_1 < D \leq D_2 \\ 1 & D \leq D_1 \end{cases} \quad (16)$$

where the relative distance (D) indicates the risk of collision between ships from a spatial perspective. The smaller the relative distance, the worse the operation effectiveness. When performing steering operations, the closer between the two ships, the smaller the change in $DCPA$, as well as the higher the probability of collision. D_1 represents the minimum distance to be avoided by the give-way ship taking emergency avoidance action. The value of D_1 generally depends on the size of the give-way ship and its maneuverability. It is generally set to be 12 to 14 times the ship length. The empirical formula for D_2 [54], which is a safe distance to give way to a ship for collision avoidance, is as follows:

$$D_2 = 1.7 \times \cos(a_{OT} - 19^\circ) + \sqrt{4.4 + 2.89 \times \cos^2(a_{OT} - 19^\circ)} \quad (17)$$

(4) The membership of a_{OT} :

$$u(a_{OT}) = \frac{1}{2} \left[\cos(a_{OT} - 19^\circ) + \sqrt{\frac{440}{289} + \cos^2(a_{OT} - 19^\circ)} \right] - \frac{5}{17} \quad 0^\circ \leq a_{OT} \leq 360^\circ \quad (18)$$

where a_{OT} represents the relative bearing of the TS [32]. The influence of relative bearing on the collision risk index is mainly related to the ease of taking collision avoidance actions. If there is no apparent change in the compass bearing of the incoming ship, it should be assumed that there is a risk of collision. Moreover, the psychological impact of the different bearing on the OOW should be taken into account. The TS is more dangerous when it is on the starboard side of the ship than on the port side and more dangerous when it is in forward of the beam than aft of the beam. Generally speaking, the risk is the largest when the relative bearing of the TS is coming from 19° of the OS with other conditions unchanged [54].

(5) The membership of K [45]:

$$u(K) = \frac{1}{1 + \frac{2}{K\sqrt{K^2+1}+2K\sin C}} \tag{19}$$

$$\sin C = |\sin(|\theta_T - \theta_0|)| \tag{20}$$

where θ_T and θ_0 are the course of the TS and the OS, respectively. Besides, $C \in [0, 180]$ is a constant coefficient [32].

The membership functions of $DCPA$ and D reveal the spatial complexity of the collision risk, and the membership function of $TCPA$ reflects the time complexity of the collision risk. α_{OT} and K are associated with the difficulty of the ship in avoidance of collision and, also, affect the psychology of the OOW.

Based on the above definition, the collision risk between two ships at time t can be obtained based on the fuzzy method. The collision risk model is defined as follows [45]:

$$f_{CRI} = W \cdot U = \left(w_{DCPA}, w_{TCPA}, w_D, w_{\alpha_{OT}}, w_K \right) \begin{bmatrix} u_{DCPA} \\ u_{TCPA} \\ u_D \\ u_{\alpha_{OT}} \\ u_K \end{bmatrix} \tag{21}$$

where f_{CRI} is the collision risk function, and U is the matrix of the membership function of the target factor, which outputs the collision risk model. W is the weight matrix, which belongs to $(0,1)$, and the sum of them is 1. w_{DCPA} , w_{TCPA} , w_D , $w_{\alpha_{OT}}$ and w_K are the set weights of the membership functions, which are usually set as 0.400, 0.367, 0.133, 0.067 and 0.033, respectively [45]. In addition, a negative $TCPA$ indicates that the two ships have passed each other.

2.2. COLREGs

COLREGs are maritime traffic regulations developed by the International Maritime Organization (IMO) to prevent and avoid collisions between ships at sea [9]. According to the COLREGs, the encounter situations of the ship are divided into three categories based on the relative bearing of the TS, e.g., head-on, overtaking and crossing. As shown in Figure 2, with the OS as the center, when the relative bearing of the TS belongs to $a_{OT} \in [0^\circ, 5^\circ] \cup [355^\circ, 360^\circ]$, it is treated as the head-on encounter situation in region F. Similarly, $a_{OT} \in [5^\circ, 67.5^\circ]$ and $a_{OT} \in [67.5^\circ, 112.5^\circ]$ represent large and small angle crossing encounter situations on the starboard side in regions A and B, respectively. Finally, $a_{OT} \in [247.5^\circ, 355^\circ]$ represents the crossing encounter situation on the port side in regions D and E.

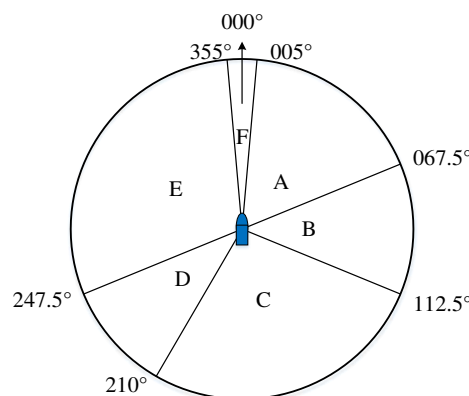


Figure 2. The classification of different ship encounter scenarios.

The ship’s responsibility to avoid collisions is divided into two categories under rules 15 and 16 of the COLREGs. When the OS is on the starboard side of the TS, the OS is a stand-on ship and should keep its course and speed. Otherwise, the OS is a give-way ship, which is responsible for avoidance and usually manoeuvres to steer to avoid collision. Moreover, the OS should not cross from ahead of the TS. The rules are not specific to the various encounter situations. Therefore, Zhang et al. [41] proposed a specific decision method for the encounter situations of large and small angle crossings, which is a good way to simplify ship avoidance decisions in multi-ship encounters, i.e., the change of course for large crossing angles and the change of speed for small crossing angles.

3. Collision Avoidance Procedure

3.1. DCPA Calculation with Course Alteration

At all stages of the ship voyage, the ship can obtain ship dynamics data such as speed, course, position and relative motion parameters through AIS, APRA and other sensors in real-time mode. It is vital to always maintain a safe distance from the TS in ship trajectory planning. DCPA is one of the key indicators to assess the overall performance of the planned trajectory. However, it should be noted that the ships may change their courses during collision avoidance operations, which would influence the calculations of the DCPA values. This issue should be considered appropriately.

During ship collision avoidance, the ship that needs to take action, whether changing course or speed, needs to stay sufficiently away from the TS to the OS. This means that the value of the DCPA should always be larger than the safe distance after the collision avoidance risk is activated. For instance, after the collision risk initiation, the whole process of the collision avoidance operation between ship 1 and ship 2 is shown in Figure 3. There are three phases, as discussed below.

1. d1 (from Ts to T2): This period is the whole process from the starting of Ship 2’s changing course to the end. In addition, both ships are changing course.
2. d2 (from T2 to T3): From the end of ship 2’s changing course to ship 1’s changing course, while ship 2 has returned to its original course.
3. d3 (from T3 to T4): Ship 1 has changed course sufficiently. Both ships have returned to their original course at this stage, while the collision avoidance operation is done.

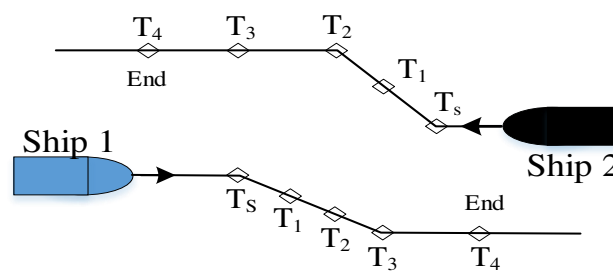


Figure 3. Closest point of approach (CPA) computation for two planned trajectories.

Assuming the OS’s initial position is (x_0, y_0) and the initial position of the TS is (x_T, y_T) , their initial speed and course are V_0, θ_0 and V_T, θ_T , respectively.

The position of the OS after time t is as follows [41]:

$$P_1(t) = (x_1(t), y_1(t)) = (x_0 + V_0 t \sin \theta_0, y_0 + V_0 t \cos \theta_0) \tag{22}$$

The position of the TS after time t is as follows [41]:

$$P_2(t) = (x_2(t), y_2(t)) = (x_T + V_T t \sin \theta_T, y_T + V_T t \cos \theta_T) \tag{23}$$

Therefore, the relative distance between the two ships after time t is as follows [41]:

$$D(t) = \left| P_1(t)P_2(t) \right| = \sqrt{(x_1(t) - x_2(t))^2 + (y_1(t) - y_2(t))^2} = \sqrt{At^2 + Bt + C} \quad (24)$$

where

$$\begin{aligned} A &= (V_0 \sin \theta_0 - V_T \sin \theta_T)^2 + (V_0 \cos \theta_0 - V_T \cos \theta_T)^2 \\ B &= 2[(x_0 - x_T)(V_0 \sin \theta_0 - V_T \sin \theta_T)^2 + (y_0 - y_T)(V_0 \cos \theta_0 - V_T \cos \theta_T)^2] \\ C &= (x_0 - x_T)^2 + (y_0 - y_T)^2 \end{aligned} \quad (25)$$

As above, the minimum value of D is the bottom of the quadratic function, which corresponds to the time t when taken to the minimum value, as follows:

$$t_{cpa} = -\frac{(x_0 - x_T)(V_0 \sin \theta_0 - V_T \sin \theta_T) + (y_0 - y_T)(V_0 \cos \theta_0 - V_T \cos \theta_T)}{(V_0 \sin \theta_0 - V_T \sin \theta_T)^2 + (V_0 \cos \theta_0 - V_T \cos \theta_T)^2} \quad (26)$$

In practice, multi-ship encounter situations are common. The *DCPA* is used as the basis for collision-avoidance decisions, and the real-time *DCPA* system calculates the relative distance between ships. In the case of changing the speed of the voyage for collision avoidance, one only needs to change the speed value in the equation.

As shown in Figure 2, according to the COLREGs, when there is a TS on the starboard side of the OS in an encounter situation, it should give way to the TS. Otherwise, the OS is a stand-on ship and should keep the initial speed and course. In this section, the procedure is also designed to ensure that giving-way ships take a more effective approach to collision avoidance in the same amount of time. In accordance with the COLREGs and good seamanship, as well system design requirements, the procedure is mainly based on changing the course and changing the speed. When necessary, the procedure is activated, and the program is shown in Figure 4.

3.2. Procedures for Changing Course Decisions

Generally, a giving-way ship to avoid collision by changing course is a major part of the procedure and is also suggested by the rules. In this part of the procedure, the focus is on the course change range and the time range of the course change. The ships are capable of safely avoiding collision under the prevailing circumstances and avoiding the end of the collision. However, it should be noted that, when the ship changes course too much or sails on the new course for too long, the ship's trajectory will deviate too much from its original trajectory, which is also undesirable. Therefore, the procedure sets the maximum and minimum values of the relevant parameters in this paper, e.g., the range of change of the course is set for 25° to 45°; the navigation time on the new course is set to 3 to 10 min. Meanwhile, we need to make sure that the TS can see the actions taken by our ship. Therefore, the change of the course amplitude and steering time should not be too small, either. Therefore, the proposed course change procedure is able to select the optimal offset and the number of decisions as far as possible in accordance with good seamanship while ensuring safety.

3.3. Procedures for Changing Speed Decisions

When a small steering angle is required to avoid collision, reducing the speed may be a more effective way to avoid the collision [41]. Therefore, when there is a small crossing angle encounter situation between the two ships, it is designed to avoid collision by reducing the speed in this paper. When it is judged necessary to activate a change of the speed program, the speed will be reduced by 5% each time to update the calculation of the closest point of approach (CPA) until it is possible to provide an effective enough way to avoid the collision between the two ships. Allow more space and time for avoidance actions. When the owned ship as a giving-way ship is encountering another ship with a small crossing angle, it is better to take the decision of changing speed rather than changing course. Therefore, the deceleration procedure is another part of the decision-making procedure.

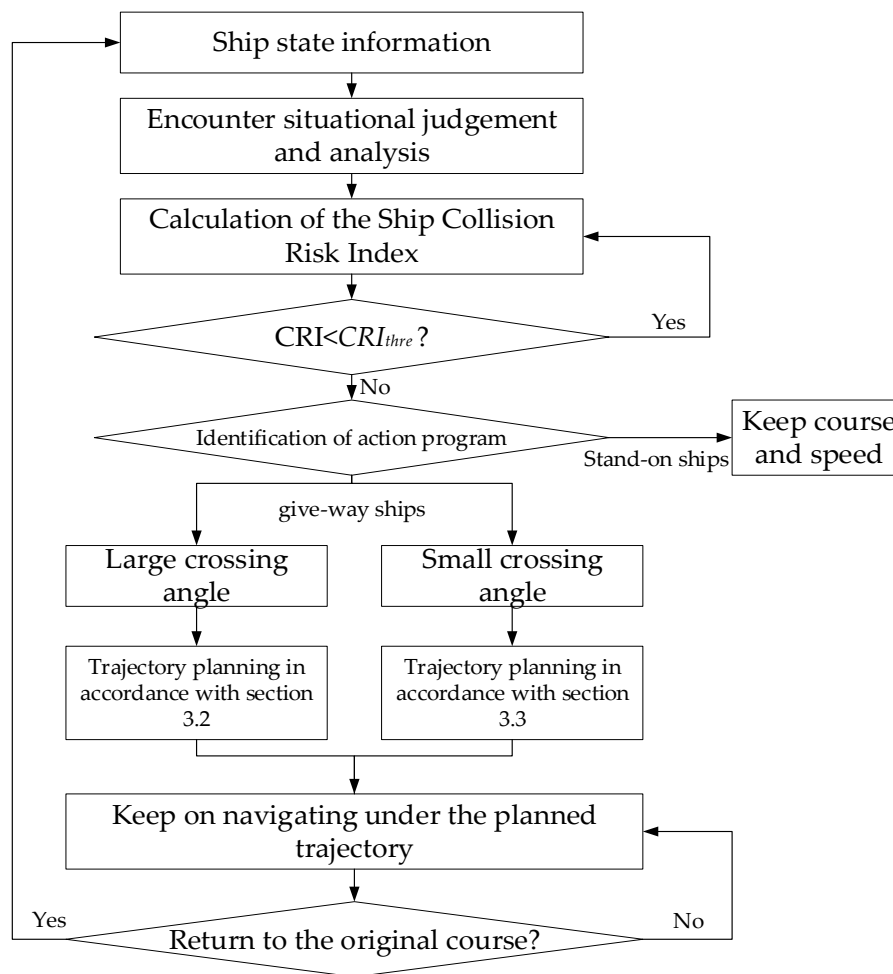


Figure 4. Trajectory planning procedure for the own ship (OS). Where *CRI* represents collision risk index, CRI_{thre} refers to collision risk index thresholds.

3.4. Real-Time Decision Support Procedure

In order to perform a distributive collision avoidance decision-making procedure, the procedure is used individually for each ship. Ships can use navigational aids to obtain static and dynamic information on the nearby ships. Based on the ship dynamics information, the real-time collision risk index is calculated. The decision is activated when the collision risk index of the two ships exceeds the threshold, and the procedure is used separately for each ship. At the same time, the real-time collision avoidance decision procedure automatically selects a decision to change course or change speed based on the angle of the encounter. On the contrary, when the real-time *CRI* does not exceed the collision threshold, the ships would keep their courses and speeds while monitoring the environment. In practice, collision avoidance manoeuvres between ships are usually one-off. The risky situation can best be defused by a single change of course or speed [41]. Therefore, it is essential to avoid taking a series of small manoeuvres to avoid collision, which is not recommended by the rules. It should be noted that the designed procedure assumes the ship returns to its original course when it finishes collision-avoidance operations. This strategy is widely accepted in open waters. This can also explain that the deviation of the ship’s course caused by steering to avoid the collision is negligible compared to the entire distance travelled by the ship from a macro perspective. After the collision avoidance is completed, the ship will continue on the new track to determine the collision risk index of nearby ships in real-time until the end of the voyage.

4. Case Studies

In this section, the effectiveness of the proposed approach is evaluated through a series of simulation experiments. The *CRI* value is tested through comparison simulations under the same encounter situations. Table 1 represents the initial multi-ship encounter scenario among four ships. The ships in such encounter scenario would collide with each other without taking any collision avoidance action. The encounter scenario consists of four ships, and the initial conditions include the position, speed, course and *CRI* of the ships.

Table 1. Parameters of the initial multi-ship encounter situation.

Ship	Ship1 (Red)	Ship2 (Green)	Ship3 (Blue)	Ship4 (Black)
Position (n mile)	(0, -4)	(2.723, 1.635)	(3.079, -1.238)	(-1.333, 3.389)
Course(deg)	0	230	300	150
Speed (kn)	18	16	16	12
collision risk index		0.4624	0.5459	0.4373

Ships are compliant with COLREGs and good seamanship in collision avoidance decision-making. In the simulations, real-time decisions are made using the proposed *CRI* approach. The decision action procedure switches between course alteration and speed change due to different crossing angles. It achieves a better collision avoidance effect in a shorter period of time and improves the efficiency of collision avoidance.

In the next subsection, the performance of the proposed collision-avoidance decision procedure based on the *CRI* is evaluated by simulations and correlation analyses of scenarios under different *CRI* thresholds.

4.1. Simulation Scenario 1

In order to better present the specifics of the ship’s collision avoidance behaviors, some details of the ships’ decision are shown in Table 2, which presents the specific operations for a ship with a *CRI* threshold of 0.6, e.g., the time of starting to changing course, speed and the new heading; the amount of course change and the nearest relative distance of ship 1 from the other ships, as well as the corresponding moment. Figure 5 shows the typical ship trajectories and positions from the simulations at several typical time points.

Table 2. Actions taken by each ship in scenario 1.

Ship	Ship 1	Ship 2	Ship 3	Ship 4
The time to start changing course (s)	282		194	625
Turning angle (deg)	33		30	25
Period of staying on the new angle (s)	405		597	158
The time to start changing speed (s)	689		2	
Period of staying on the new speed (s)	812		1498	
Percentage of initial speed (%)	60		70	
Nearest relative distance of the other ship (nm) and moments		0.91 706	0.86 1133	0.88 1105

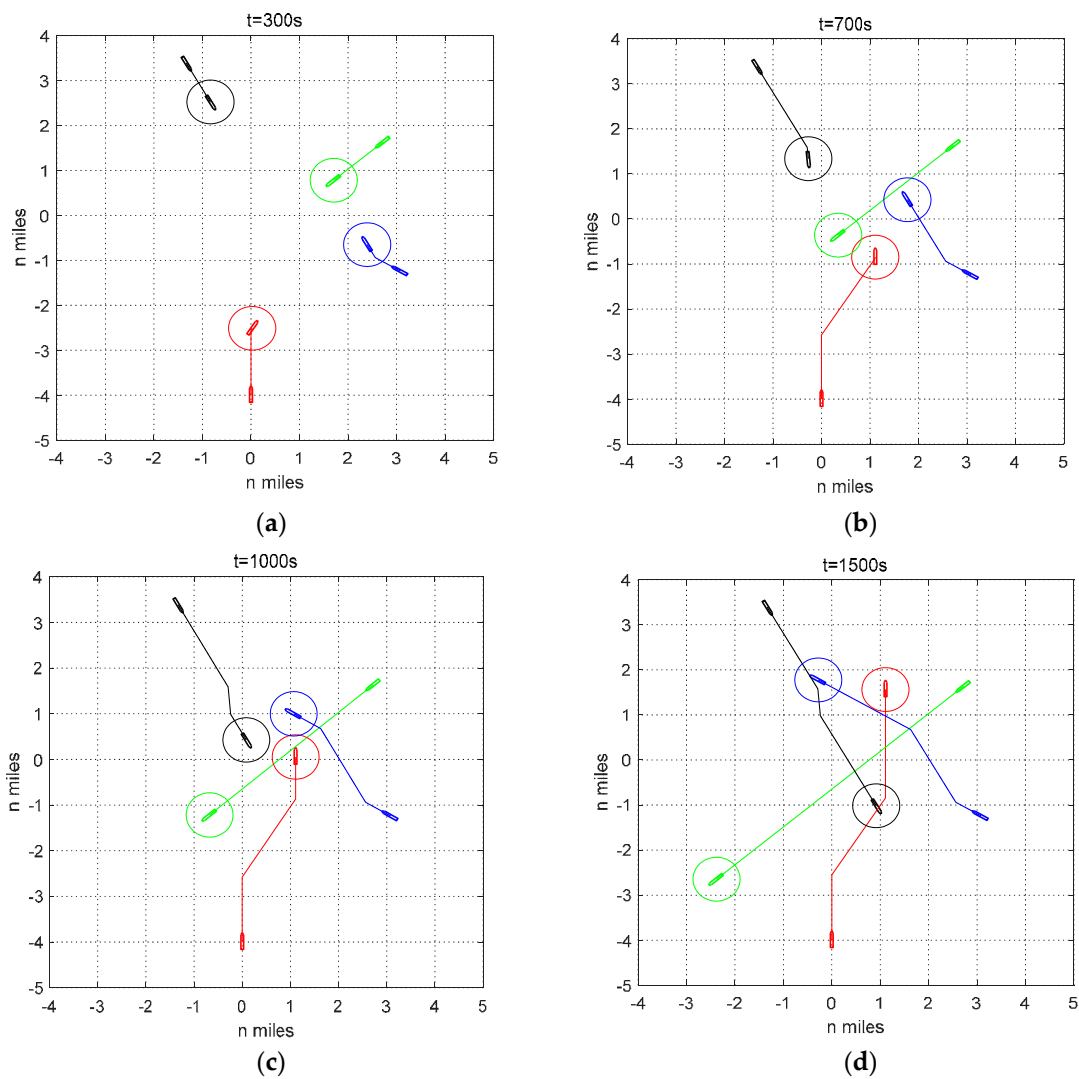


Figure 5. Ships’ trajectories under scenario 1: (a) the positions and paths of ships at 300 s, (b) the positions and paths of ships at 700 s, (c) the positions and paths of ships at 1000 s and (d) the positions and paths of ships at 1500 s.

Table 2 and Figure 5 show the positions and paths of the simulation ships involved in the experiment. When $t = 2$ s, S_3 makes the first decision and operation when it encounters S_2 with a small crossing angle. S_3 reduces speed by 30% and keeps for 1498 s. Besides, S_3 also encounters S_4 with a large crossing angle. S_3 is on the port side of S_4 . Therefore, she turns to starboard for 30° and keeps for 597 s on the new course. Similarly, since S_1 and S_2 are encountered with a large crossing angle, S_1 makes the decision of turning to the starboard by 33° and keeps on the new course for 405 s. As shown in Figure 6a,d, the *DCPA* of S_1 with S_2 , S_3 and S_4 increases, and the real-time *CRI* of S_1 with S_2 and S_4 decreases. S_1 reduces the speed to 60% of the initial speed to pass the aft of S_3 at $t = 689$ s, which is also stipulated by COLREGs and good seamanship. According to Figure 6a, the *CRI* between S_1 and S_2 is significantly lower at 282 s and 689 s, indicating that the action is beneficial for collision avoidance. At last, S_4 encounters S_1 with a large crossing angle at 625 s. S_4 turns 25° to starboard and keeps the new course for 158 s. As shown in Figure 6b, the *TCPA* values between S_1 and the other ships were changed to negative at 687 s, 1134 s and 1103 s, respectively, which indicates that the collision avoidance actions are effective. In the simulation, S_2 did not take any actions. According to the distributed multi-ship collision avoidance and COLREGs, although S_2 is on the port side of S_4 ,

they did not incur a collision risk in this scenario. In this simulation, each ship’s collision avoidance actions are helpful and do not increase the collision risk.

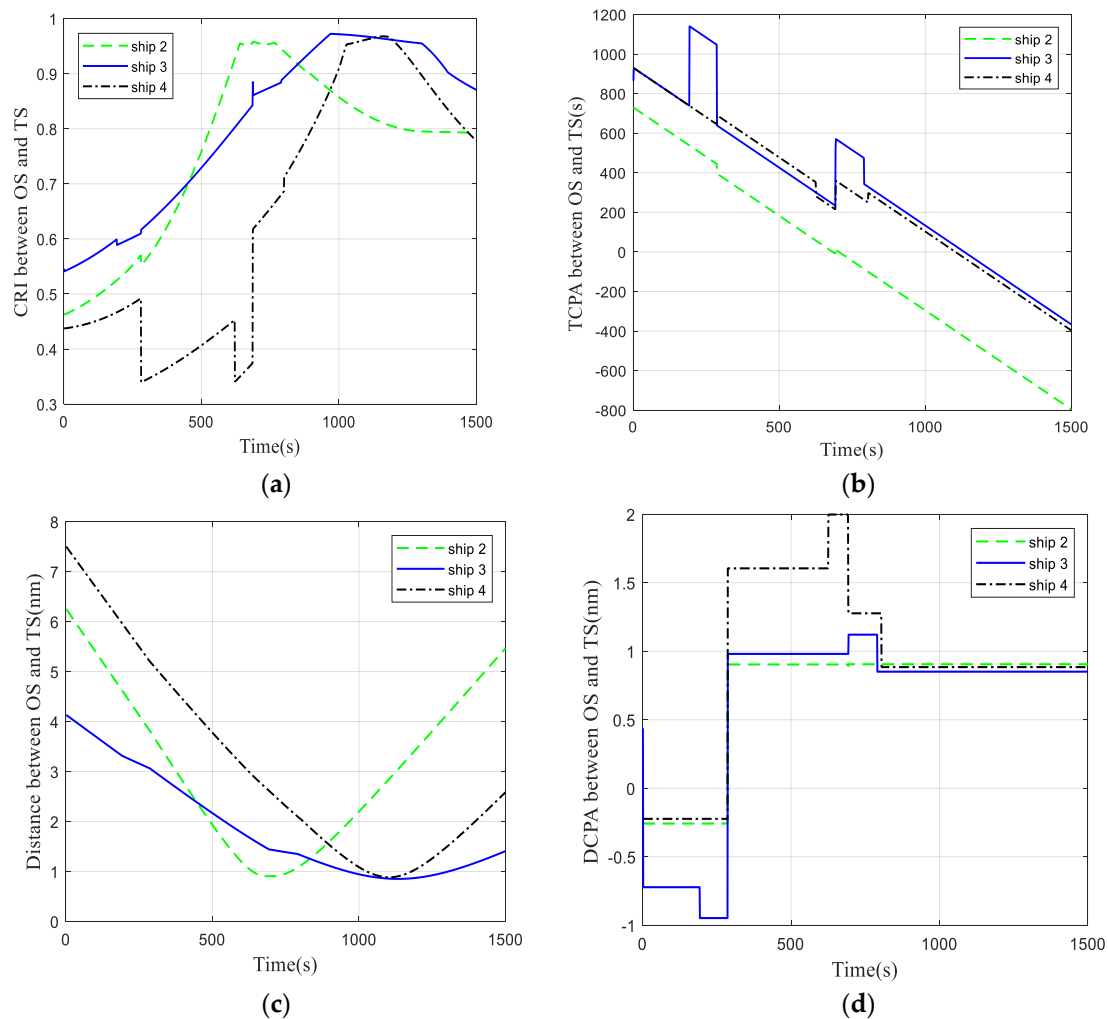


Figure 6. Real-time parameter changes under scenario 1: (a) the collision risk index (*CRI*) with the Target Ships (TSs), (b) the time to the closest point of approach (*TCPA*) with the TSs, (c) the relative distance with the TSs and (d) the distance to the closest point of approach (*DCPA*) with the TSs.

4.2. Simulation Scenario 2

In this scenario, the threshold of the *CRI* is set to 0.7 in the simulations. Figure 7 shows the trajectories and positions of the ships at several typical time points.

In this simulation, it can be seen that the ships’ collision avoidance actions shown in Figure 7 and Table 3 are delayed compared with the first simulation. When $t = 429$ s, S_1 encounters S_2 with a large crossing angle, and the *CRI* is equal to 0.7 in Figure 8. S_1 turns 40° to starboard and keeps on the new course for 599 s. As shown in Figure 8a,d. The real-time *CRI* of S_1 and S_2 and S_4 are reduced at 429 s. Meanwhile, S_1 makes the decision of turning to the starboard and the stern of S_3 , which results in a slight increase in the collision risk index with S_3 . The *DCPA* value of S_1 with the other ships is increased in Figure 8d. S_3 encounters S_2 with a small crossing angle at 77 s. S_3 reduces the speed for 35% and keeps on for 1424 s. S_3 and S_4 form a large crossing angle encounter situation; thus, S_3 is turning to the starboard by 32° and remains on the new heading for 581 s. In Figure 8b, the *TCPA* values between S_1 and the other ships change to negative at 687 s, 1134 s and 1103 s, respectively.

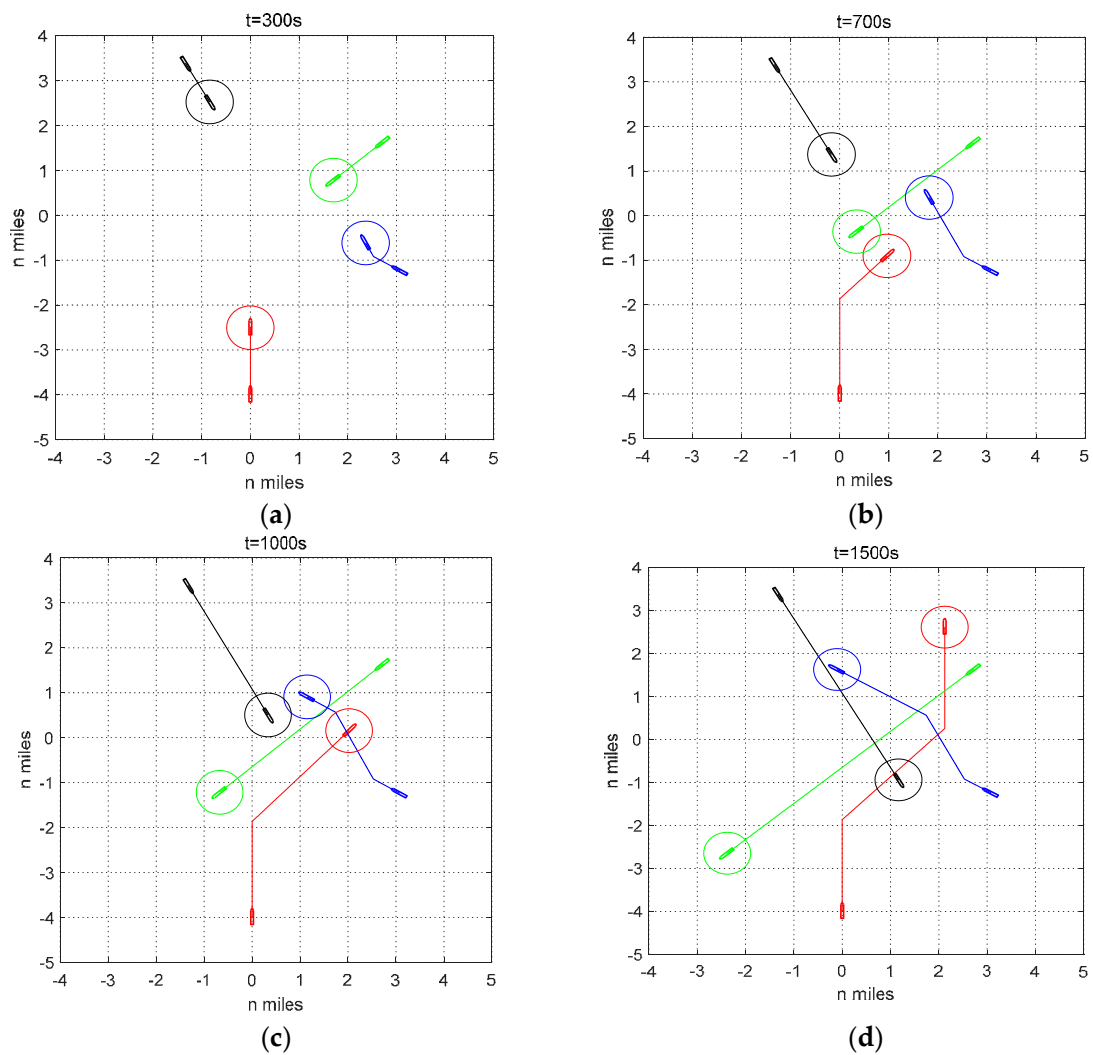


Figure 7. Ships’ trajectories under scenario 2: (a) the positions and paths of ships at 300 s, (b) the positions and paths of ships at 700 s, (c) the positions and paths of ships at 1000 s and (d) the positions and paths of ships at 1500 s.

Table 3. Actions taken by each ship under scenario 2.

Ship	Ship 1	Ship 2	Ship 3	Ship 4
The time to start changing course (s)	429		182	625
Turning angle (deg)	40		32	25
Period of staying on the new angle (s)	599		581	158
The time to start changing speed (s)			77	
Period of staying on the new speed (s)			1424	
Percentage of initial speed (%)			65	
Nearest relative distance of the other ship (nm) and moments		0.82 690	1.05 959	1.68 1100

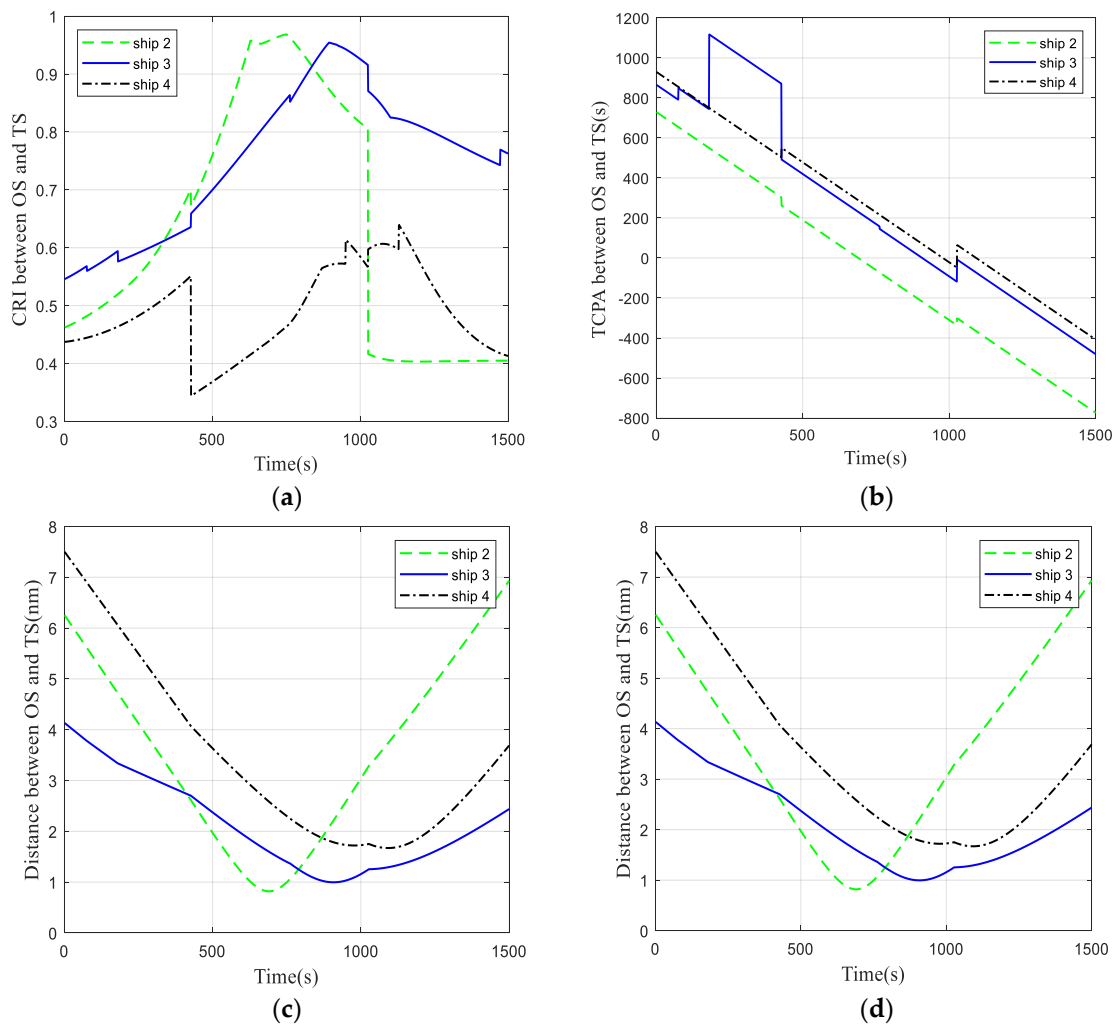


Figure 8. Real-time parameter changes under scenario 2: (a) the collision risk index (*CRI*) with the Target Ships (TSs), (b) the time to the closest point of approach (*TCPA*) with the TSs, (c) the relative distance with the TSs and (d) the distance to the closest point of approach (*DCPA*) with the TSs.

4.3. Simulation Scenario 3

In this simulation, the threshold of the *CRI* for all ships is set to 0.9 for the collision avoidance decision-making procedure given the same encounter situations. The trajectories of the four ships and their positions at typical time points are shown in Figure 9.

According to the data of Table 4, S_3 encounters S_4 with a large crossing angle at 309 s, which turns 40° to starboard and keeps on the new angle for 599 s. Meanwhile, S_3 also encounters S_4 with a small crossing angle at 309 s. S_3 reduces the speed to 45% of the initial speed. Similarly, when $t = 577$ s, S_1 turns 45° to starboard to avoid S_2 . As shown in Figure 10a,d, the *DCPA* values of S_1 and S_2 , S_3 and S_4 are increased, and the *CRI* values of S_1 and S_3 and S_4 decrease at 577 s, but due to the late change of course, the *CRI* values of S_1 and S_2 continue increasing. The *TCPA* values between S_1 and S_2 , S_3 and S_4 change to negative at 716 s, 994 s and 970 s in Figure 10b, respectively. The collision avoidance actions undertaken by the ships are effective. However, S_1 takes a large angle to change course in Figure 9. In the collision avoidance decision when the threshold of the *CRI* is 0.9, the ships are not properly coordinated, and the actions between the ships are relatively passive, which results in this scenario are much more difficult than scenario 1 and 2. Therefore, the highest risky situation occurs at 715 s in this scenario, when the distance between S_1 and S_2 is 574 m in Figure 10c. Although the two ships are

almost parallel with the opposite course, it is still an undesirable situation. This is due to the large threshold value results in the late decision to perform a collision-avoidance action.

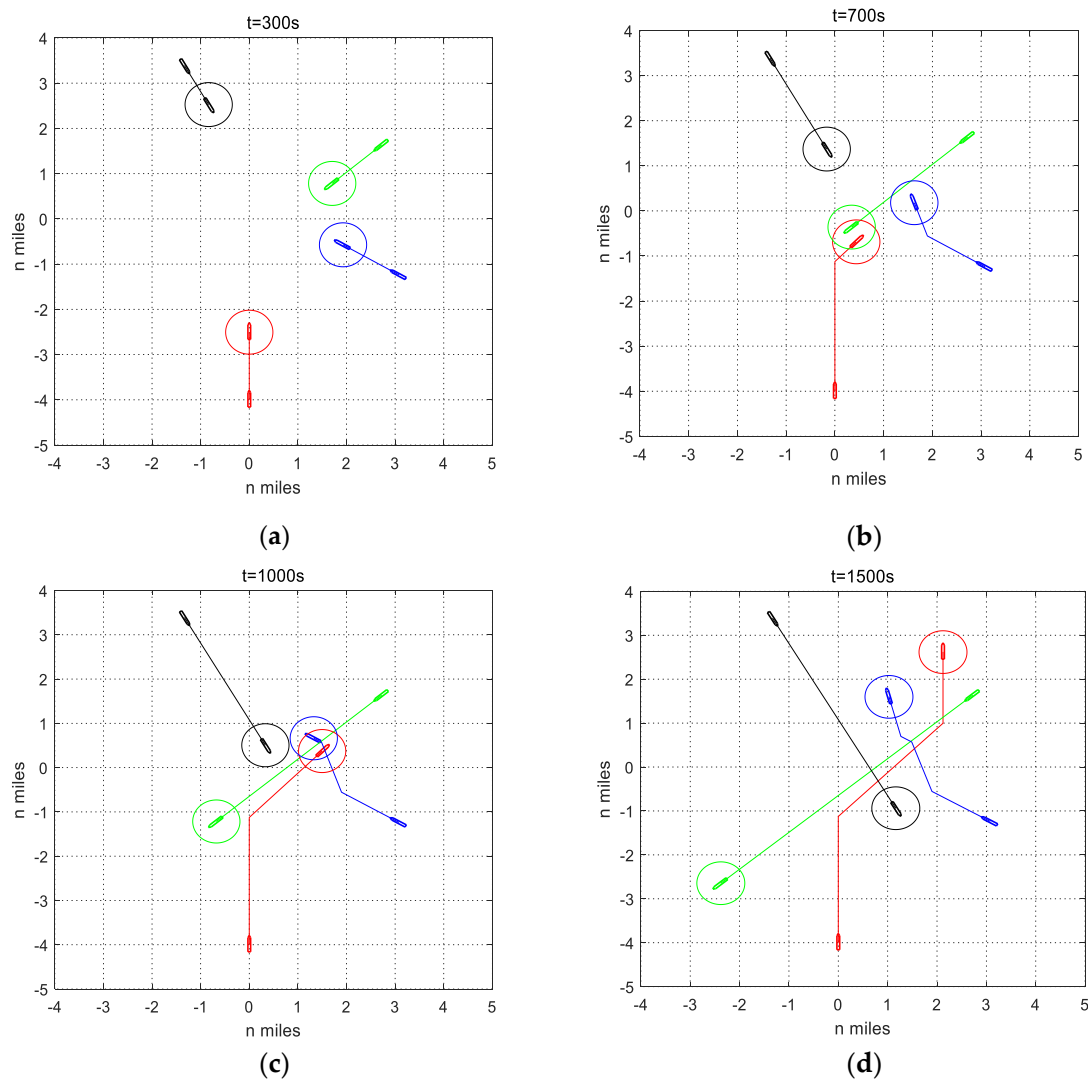


Figure 9. Ships’ trajectories under scenario 3: (a) the positions and paths of ships at 300 s, (b) the positions and paths of ships at 700 s, (c) the positions and paths of ships at 1000 s and (d) the positions and paths of ships at 1500 s.

Table 4. Actions taken by each ship in scenario 3.

Ship	Ship 1	Ship 2	Ship 3	Ship 4
The time to start changing course (s)	577		309	
Turning angle (deg)	45		40	
Period of staying on the new angle (s)	598		599	
The time to start changing speed (s)			309	
Period of staying on the new speed (s)			1191	
Percentage of initial speed (%)			45	
Nearest relative distance of the other ship (nm) and moments		0.31 715	0.34 990	1.16 968

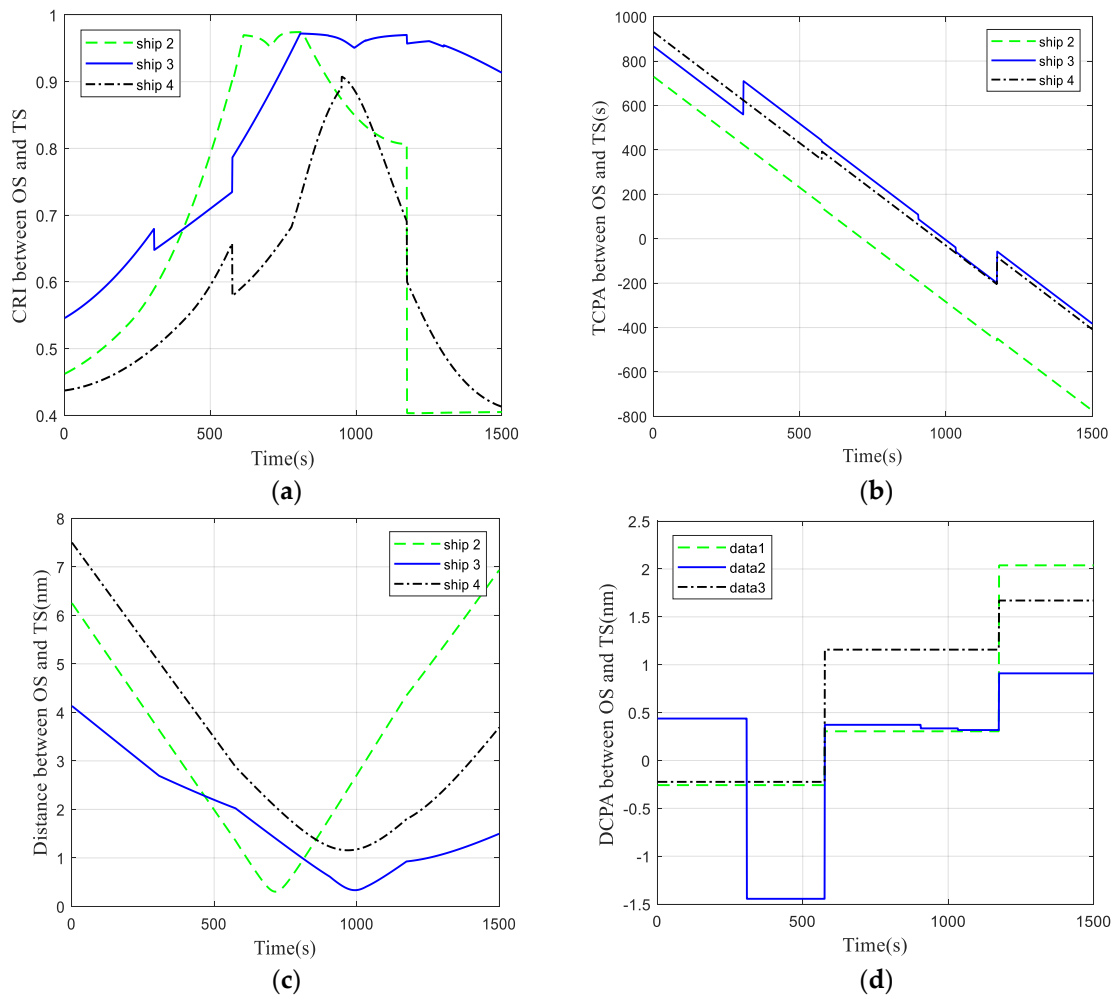


Figure 10. Real-time parameter changes under scenario 3: (a) the collision risk index (*CRI*) with the Target Ships (*TSs*), (b) the time to the closest point of approach (*TCPA*) with the *TSs*, (c) the relative distance with the *TSs* and (d) the distance to the closest point of approach (*DCPA*) with the *TSs*.

4.4. Simulation Scenario 4

It should be noted, in this scenario, that when facing with the same encounter scenario, the *CRI* selected by different *OOWs* during collision avoidance decision-makings may vary a lot due to their different navigational experience and their different psychological states, as well as other types of influencing factors. That is to say, the *OOWs* may make different decisions in the same encounter scenario. Therefore, the thresholds of different *CRI* values are applied to the four encounter ships during the collision avoidance decision-making to verify the performance of the proposed approach. The trajectories and positions of the simulated ships at typical time points are presented in Figure 11.

Table 5 and Figure 12 illustrate the ships' action details and Parameter changes. Since each ship selects different thresholds, the results are quite different from scenarios 1–3. At $t = 233$ s, S_1 and S_3 encounter each other with a small crossing angle, while S_1 and S_2 encounter with a large crossing angle. S_1 turns 25° to starboard and reduces to 85% of its original speed. The collision risk reference threshold for S_1 is 0.6, and the timing of the action is seen to be on time, i.e., the steering and speed range are relatively small. When $t = 732$ s, S_1 makes the decision to continue to reduce speed in order to safely sail from aft of S_3 and reduces the speed to 45% of the original speed. Similarly, S_3 encounters at a large crossing angle with S_4 and a small crossing angle with S_2 at 309 s. S_1 makes the decision to turn 40° to starboard, as well as navigates on the new course for 597 s, which reduces the speed to 45% of the original speed to complete the collision avoidance manoeuvre. The timing of

the decision is related to the ship’s initial position and state of motion. The decision of S_4 is the last, and its first decision occurs at 605 s, which includes turning 25° to starboard. S_4 crosses from the aft region of S_1 , and S_4 crosses from the aft region of S_1 . All the ships’ behaviors are consistent with the COLREGs. In this scenario, the higher the threshold of CRI chosen by S_3 , the greater the magnitude of the collision-avoidance manoeuver.

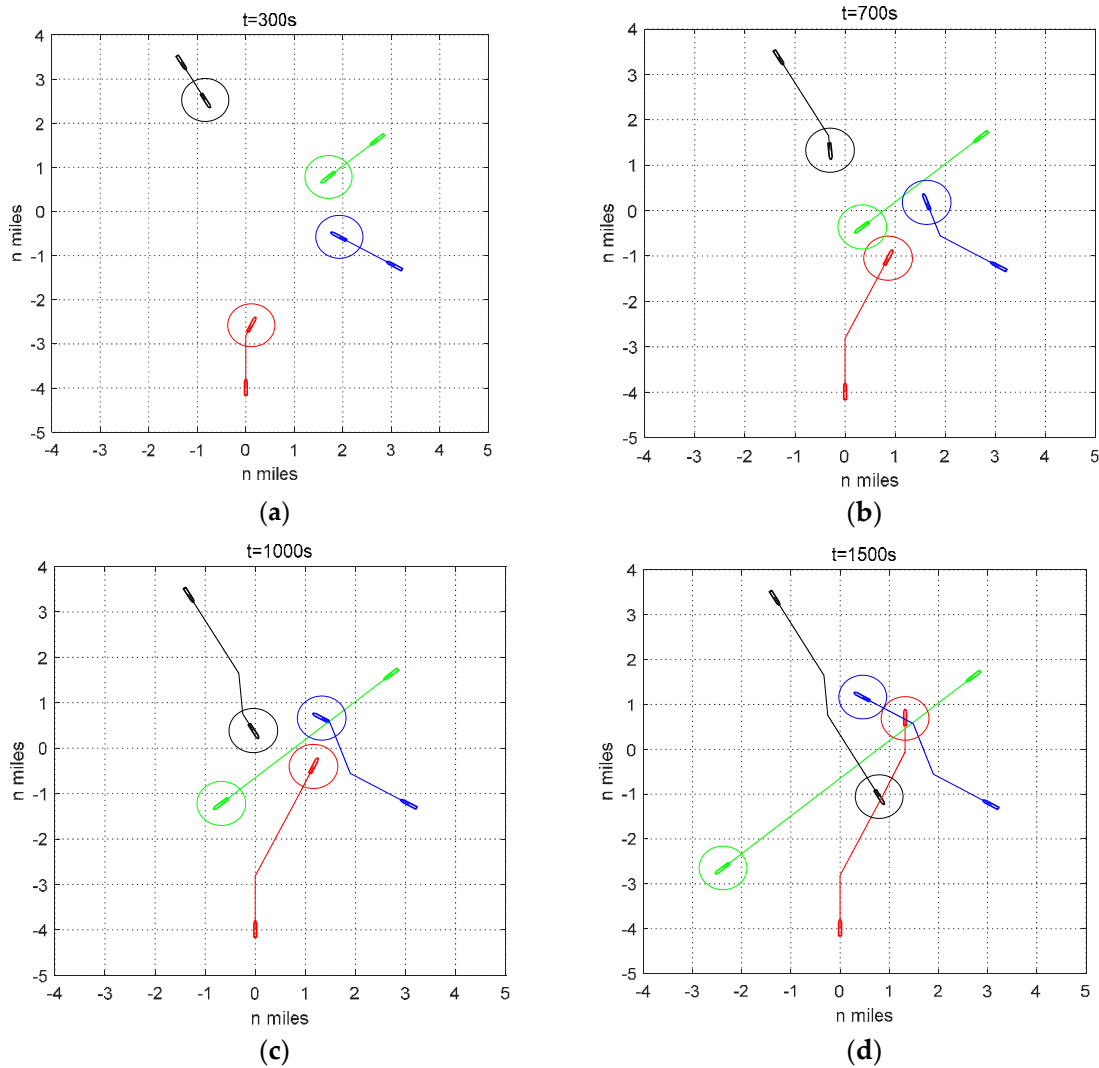


Figure 11. Ships’ trajectories under scenario 4: (a) the positions and paths of ships at 300 s, (b) the positions and paths of ships at 700 s, (c) the positions and paths of ships at 1000 s and (d) the positions and paths of ships at 1500 s.

Table 5. Actions taken by each ship in scenario 4.

Ship	Ship 1	Ship 2	Ship 3	Ship 4
The time to start changing course (s)	233		309	605
Turning angle (deg)	25		40	25
Period of staying on the new angle (s)	954		599	267
The time to start changing speed (s)	233; 732		309	
Period of staying on the new speed (s)	498; 768		1191	
Percentage of initial speed (%)	85; 45		45	
Collision risk reference thresholds	0.6	0.8	0.9	0.7

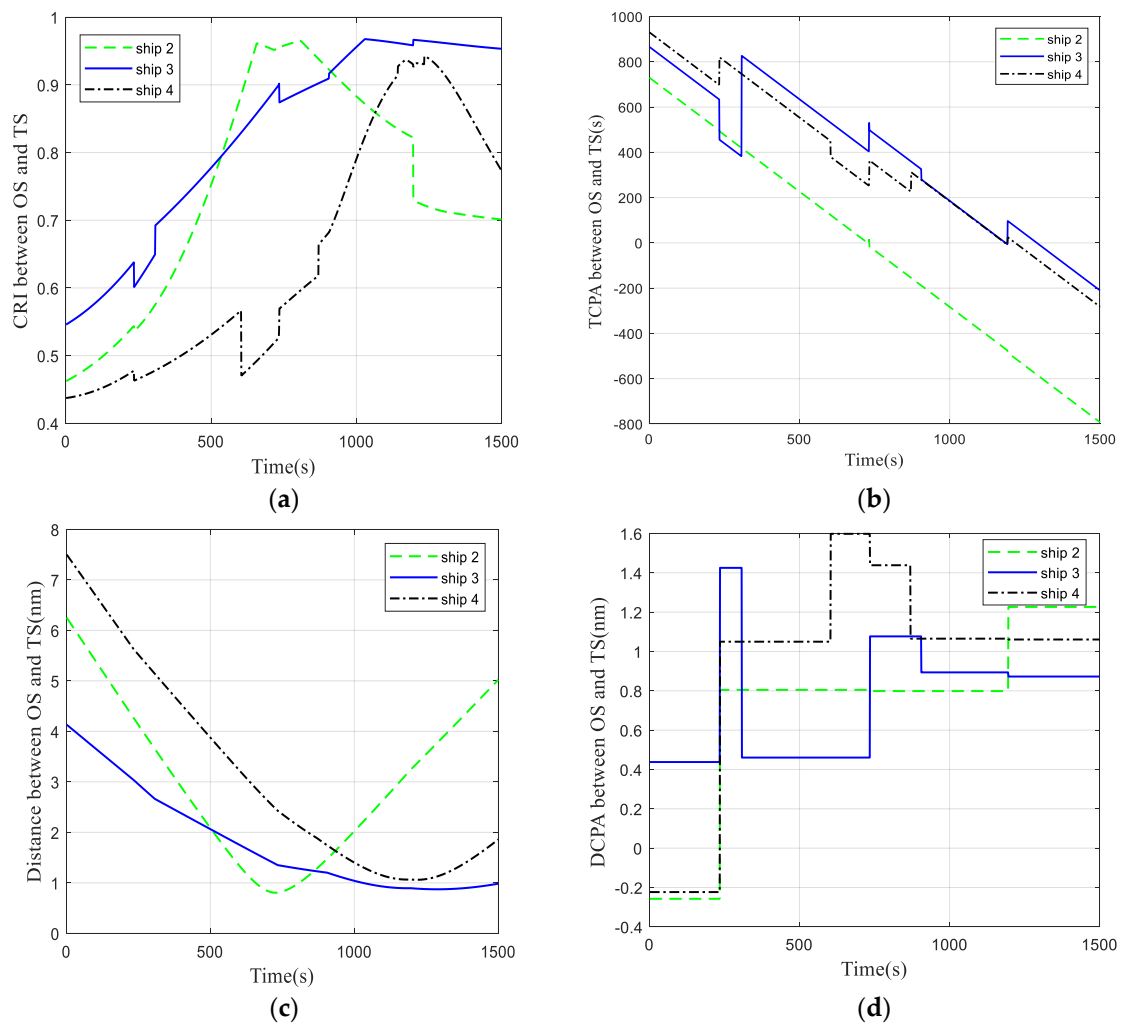


Figure 12. Real-time parameter changes under scenario 4: (a) the collision risk index (*CRI*) with the Target Ships (*TSs*), (b) the time to the closest point of approach (*TCPA*) with the *TSs*, (c) the relative distance with the *TSs* and (d) the distance to the closest point of approach (*DCPA*) with the *TSs*.

4.5. Simulation Scenario 5

In this simulation, it is supposed that the OOW of S_1 may select a larger *CRI* threshold value, and the OOW of S_4 has less experience and uses a smaller threshold value. Moreover, the reference collision risk reference threshold varies for each ship, and the simulation test is conducted to verify the effectiveness of the procedure. The trajectories of the simulated ships at typical time points is presented in Figure 13.

According to Table 6 and Figure 14, S_3 and S_2 encounter with a small crossing angle at 77 s, and S_3 reduces speed to 65% of the original speed. According to the COLREGs, S_3 should be the give-way ship of S_4 . Therefore, S_3 turns starboard to keep clear and avoid S_4 at 182 s. Similarly, S_4 turns 42° to starboard to avoid collision with S_1 and S_4 , which keeps on the new angle for 598 s. Finally, S_1 makes the decision of turning starboard for 45° to avoid collision with S_1 and S_2 . Due to the reasoning that the collision risk threshold of S_1 is large, S_1 takes the last and largest action to avoid collision, which is not recommended by the COLREGs. As shown in Figure 14a,d. The collision risk of S_1 and S_4 decrease, and the *DCPA* values of S_1 and S_2 , S_3 and S_4 increase at 577 s. In Figure 14b, the *TCPA* values between S_1 and S_2 , S_3 and S_4 reduce to negative values at 716 s, 975 s and 842 s, respectively. The relative distances of the ships are shown in Figure 14c. When the *CRI* threshold is selected as a large value, a small relative distance can occur. Even though the collision is avoided, the encounter situation is

more complicated. With higher demands on the OOWs' maneuvering levels, the OOWs are more likely to pay close attention to the ship dynamics of other ships in the vicinity.

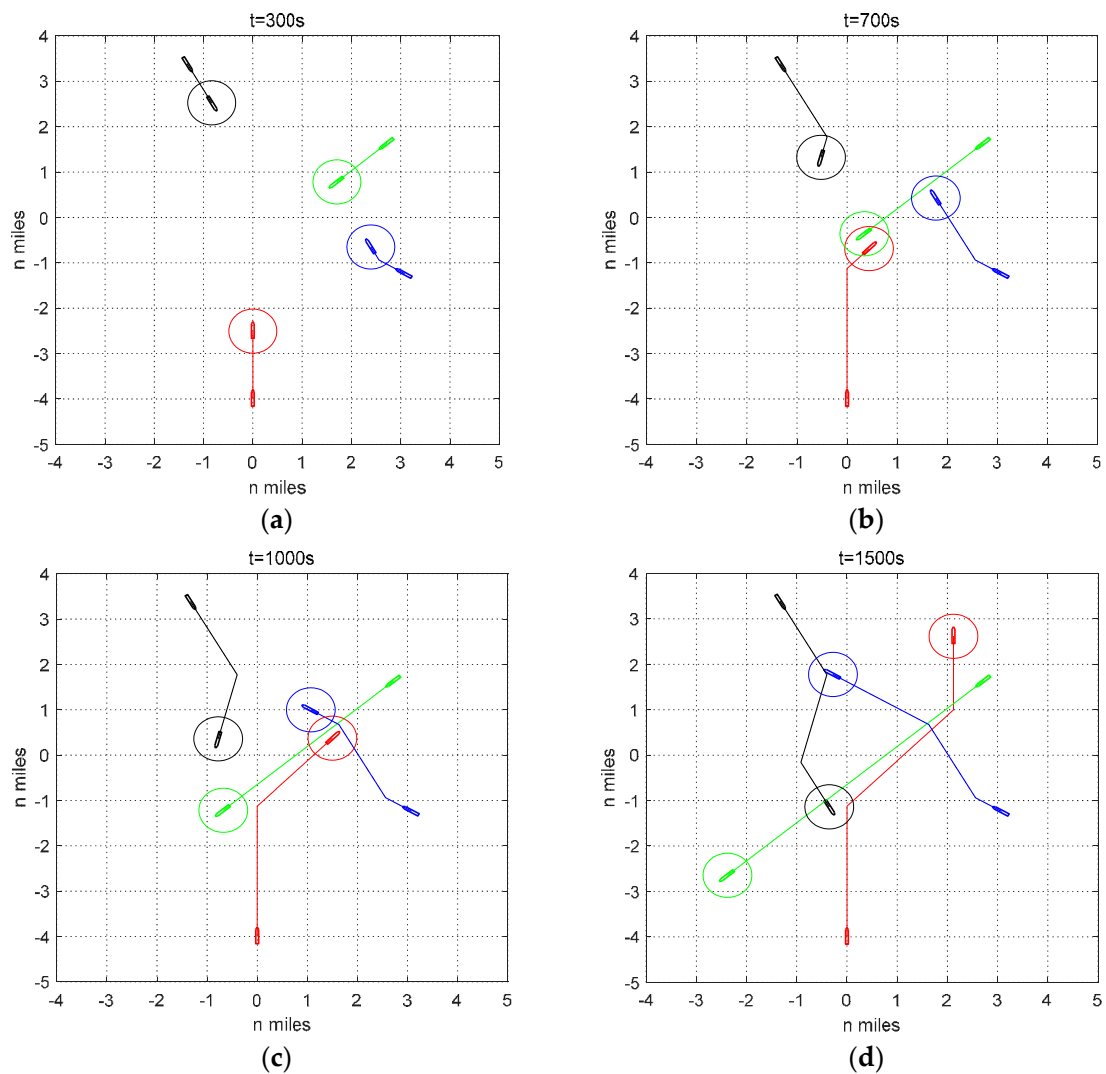


Figure 13. Ships' trajectories under scenario 5: (a) the positions and paths of ships at 300 s, (b) the positions and paths of ships at 700 s, (c) the positions and paths of ships at 1000 s and (d) the positions and paths of ships at 1500 s.

Table 6. Actions taken by each ship in scenario 5.

Ship	Ship 1	Ship 2	Ship 3	Ship 4
The time to start changing course (s)	577		182	553
Turning angle (deg)	45		32	42
Period of staying on the new angle (s)	598		581	598
The time to start changing speed (s)			77	
Period of staying on the new speed (s)			1423	
Percentage of initial speed (%)			65	
Collision risk reference thresholds	0.9	0.8	0.7	0.6

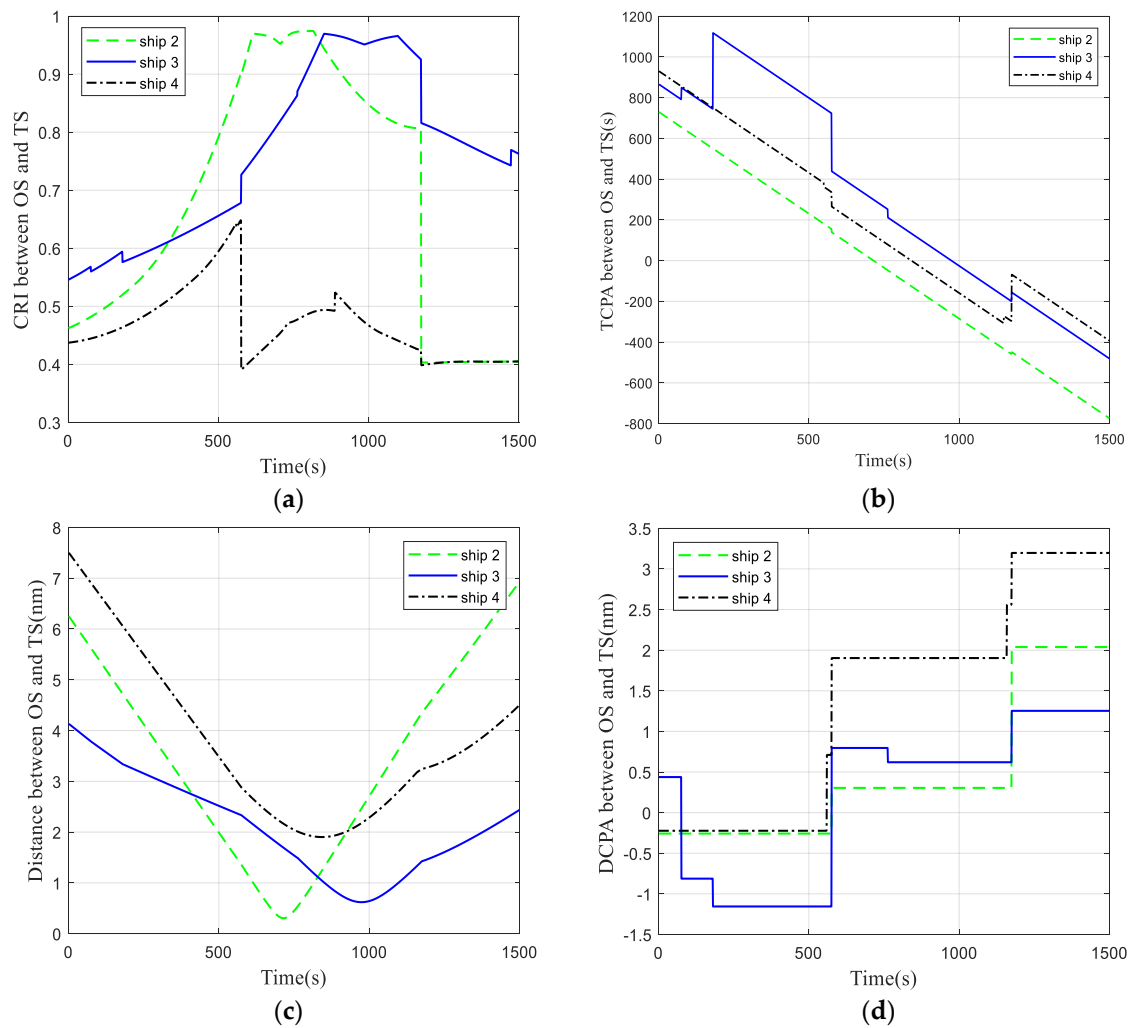


Figure 14. Real-time parameter changes under scenario 5: (a) the collision risk index (CRI) with the Target Ships (TSs), (b) the time to the closest point of approach (TCPA) with the TSs, (c) the relative distance with the TSs and (d) the distance to the closest point of approach (DCPA) with the TSs.

5. Discussion

5.1. Analysis of trajectory safety

In the above cases, when different CRI thresholds are selected, the relative distances derived from taking the decision are quite different in Figures 6c, 8c and 10c. As shown in Figure 10c, the relative distances between S_1 and S_2 and S_1 and S_3 are much smaller than those in Figures 6c and 8c with the same encounter situations. These indicate that the collision-avoidance actions of the ships are more coordinated when the CRI threshold chosen is relatively low. S_3 reduces the speed to 70% and 65% of the initial speed at $t = 2$ s and $t = 77$ s, respectively, in Tables 2 and 3. However, S_3 reduces the speed to 45% of the initial speed at 309 s in Table 4, which brings a new challenge to the ship's speed reduction maneuver. Therefore, when the reference threshold is set to 0.9, the ship is too late to make the decision to avoid collision. Safety is low, and the OOW needs to be highly alert to his surroundings and places higher demands on the ship's maneuverability.

5.2. Analysis of Trajectory Efficiency

Tables 2–4 reveal the parameters of the ships' action measures in the collision avoidance process at different reference thresholds, respectively. In Figure 5, S_1 turns 33° to starboard at 282 s and navigates

on the new heading for 405 s, while, in Figure 7, the action is taken later, i.e., S_1 turns 40° to starboard at 429 s and navigates on the new course for 599 s, due to the large *CRI* threshold.

Table 7 presents the ship maneuvering details for the experimental results of Scenarios 1–3. According to the data in Table 5, when the selected *CRI* is 0.6, S_1 's trajectory deviates 1.315 nm from the original trajectory. However, with the increase of the *CRI*, the steering angle of the ship increases as well. When the selected *CRI* are 0.7 and 0.9, S_1 's trajectory deviates 2.513 nm and 2.990 nm. That is to say, the former is more economical. Therefore, the collision risk threshold that is too high will cause the ship to deviate from the original course to a large degree. As shown in Table 7, the deviation of the track at a collision risk threshold of 0.9 is more than twice as large as the case with a threshold of 0.6. This is also not recommended by good seamanship if action is taken too late. Tables 5 and 6 present the information on ship operations for different ships that have different *CRI* thresholds. Meanwhile, ships can successfully complete collision avoidance decisions even when the reference thresholds are different in Figures 11 and 13. Besides, in both scenarios, we also find that the larger *CRI* of the selected threshold leads to a later decision and a larger magnitude of manipulation.

Table 7. Comparison of the results of scenarios 1–3.

Collision Risk Thresholds	0.6	0.7	0.9
Maximum steering angle ($^\circ$), ship	$33^\circ, S_1$	$40^\circ, S_1$	$45^\circ, S_1$
Length of deviation from route course (nm)	1.315	2.513	2.990
Reduction of speed (%)	40, S_1	35, S_3	55, S_3
Number of steering, ship	1, S_1 ; 1, S_3 ; 1, S_4	1, S_1 ; 1, S_3	1, S_1 ; 3, S_3
Number of speed changes, ship	1, S_1 ; 1, S_3	1, S_3	1, S_3

5.3. Analysis of Maneuver Difficulty

According to Tables 2–4, when the threshold is 0.6, the steering amplitude taken is relatively small. On the contrary, when the thresholds are 0.7 and 0.9, the ships take larger steering actions. In multi-ship encounter scenario, taking excessive steering actions can easily create a secondary collision risk with other ships, which would result in one more operation. In Table 4 and Figure 9, S_3 takes multiple steering actions to avoid collision. In practice, it is much more difficult for the OOW to maneuver in this scenario. Furthermore, the OOW is prone to making the wrong decisions in such a stressful encounter situation. In scenarios 4 and 5 with different *CRI* thresholds, S_3 only takes one turn and is more effective, as shown in Figures 11 and 13. In reality, it is also common for different decision-makers to choose different thresholds. If this collision risk and collision avoidance decision model is actually used on-board a ship, it can provide the OOW with the best time to make a collision avoidance decision or raise an alarm if the real-time collision risk exceeds the threshold. Moreover, the OOW can get real-time access to path planning for collision-avoidance decisions.

6. Conclusions

In this paper, a distributed multi-ship collision avoidance decision-making on the premise of satisfying the COLREGs and good shipman ship is studied, which focuses on comparing the collision-avoidance decisions made by each ship choosing the same and different collision risk thresholds from its own perspective. It compensates for the excessive subjectivity of the OOW in the decision-making process. The model can provide a potential way to harmonize collision avoidance decision-making for the OOW in dealing with multi-ship encounter situations. The results indicate that:

- (1) The timing of the ship taking collision-avoidance action is closely related to the selected value of the *CRI*. This paper evaluates the validity of the proposed multi-ship collision-avoidance decision model based on the collision risk index through five groups of comparative experiments and carries out a detailed parameter analysis and finds that, when the collision risk threshold value taken by the ship is small (such as *CRI* = 0.6), the ship takes a more timely collision avoidance

action, and the magnitude is in-line with the recommendation of the COLREGs. Therefore, through discussion and analysis, it is suggested that the threshold of the *CRI* be within (0.6, 0.7), which will also be affected by other factors such as visibility, sea state, etc. The OOWs need to adjust the *CRI* to the real-time navigational environment. Meanwhile, the OOW's experience in maneuvering ships should not be ignored as an aid to collision avoidance decision-making.

- (2) In multi-ship collision avoidance, different collision risk thresholds are set for experimentation, especially when different ships adopt different collision risk thresholds in the same scenario; the model can also provide decision aid and collision-avoidance warning for the OOW.
- (3) The fuzzy logic-based collision risk calculation method and expanding the real-time dynamic parameters such as the *CRI*, *TCPA*, *DCPA* and *D* are practical tools for a real-time collision risk analysis in multi-ship encounter situations.

Ship collision risk assessment models are the basis for collision-avoidance decisions. The integration of relevant data analysis indicators into visualization systems will be a way forward in future research. In addition, the consideration of the effects of ship maneuverability and static obstacles on collision-avoidance decisions should also be investigated as a key focus of future research.

Author Contributions: The manuscript was written by Y.H. and J.Z. All authors discussed the original idea. Conceptualization, Y.H.; methodology, Y.H. and W.T.; software, Y.H.; validation, Y.H.; formal analysis, Y.H.; investigation, Y.H.; resources, A.Z.; data curation, A.Z. and W.T.; writing—original draft preparation, Y.H. and A.Z.; writing—review and editing, A.Z. and J.Z.; visualization, Y.H. and Z.H.; project administration, A.Z. and funding acquisition, A.Z. and J.Z. All authors have read and agreed to the published version of the manuscript.

Funding: This research was funded by National key research and development program of China (2018YFC1407400), Guangxi Natural Science Foundation (2018JJB160093) and Qinzhou Science Research and Technology Development Project (20198521).

Conflicts of Interest: The authors declare no conflict of interest.

References

1. George, R. *Ninety Percent of Everything. Inside Shipping, the Invisible Industry That Puts Clothes on Your Back, Gas in Your Car, and Food on Your Plate*; Portobello Books: London, UK, 2013; ISBN 9780805092639.
2. Wu, B.; Yan, X.; Wang, Y.; Soares, C.G. An evidential reasoning-based cream to human reliability analysis in maritime accident process. *Risk Anal.* **2017**, *37*, 1936–1957. [[CrossRef](#)]
3. Baldauf, M.; Benedict, K.; Fischer, S.; Motz, F.; Schröder-Hinrichs, J.-U. Collision avoidance systems in air and maritime traffic. *Proc. IMechE* **2011**, *225*, 333–343. [[CrossRef](#)]
4. Kim, M.H.; Heo, J.H.; Wei, Y.; Lee, M.C. A path plan algorithm using artificial potential field based on probability map. In Proceedings of the 2011 8th International Conference on Ubiquitous Robots and Ambient Intelligence, Songdo Conventia, Incheon, Korea, 23–26 November 2011; pp. 41–43. [[CrossRef](#)]
5. Yıldırım, U.; Başar, E.; Uğurlu, Ö. Assessment of collisions and grounding accidents with human factors analysis and classification system (HFACS) and statistical methods. *Saf. Sci.* **2019**, *119*, 412–425. [[CrossRef](#)]
6. Fan, S.; Blanco-Davis, E.; Yang, Z.; Zhang, J.; Yan, X. Incorporation of human factors into maritime accident analysis using a data-driven bayesian network. *Reliab. Eng. Syst. Saf.* **2020**, *203*, 107070. [[CrossRef](#)]
7. Fan, S.; Zhang, J.; Blanco-Davis, E.; Yang, Z.; Wang, J.; Yan, X. Effects of seafarers' emotion on human performance using bridge simulation. *Ocean Eng.* **2018**, *170*, 111–119. [[CrossRef](#)]
8. Fan, S.; Zhang, J.; Blanco-Davis, E.; Yang, Z.; Yan, X. Maritime accident prevention strategy formulation from a human factor perspective using bayesian networks and topsis. *Ocean Eng.* **2020**, *210*, 107544. [[CrossRef](#)]
9. IMO. *Conventions on the International Regulations for Preventing Collision at Sea (COLREGs)*; The International Maritime Organization (IMO): London, UK, 1972.
10. Hilgert, H.; Baldauf, M. A common risk model for the assessment of encounter situations on board ships. *Dtsch. Hydrogr. Z.* **1997**, *49*, 531–542. [[CrossRef](#)]
11. Huang, Y.; van Gelder, P.H.A.J.M. Collision risk measure for triggering evasive actions of maritime autonomous surface ships. *Saf. Sci.* **2020**, *127*, 104708. [[CrossRef](#)]
12. Du, L.; Goerlandt, F.; Kujala, P. Review and analysis of methods for assessing maritime waterway risk based on non-accident critical events detected from AIS data. *Reliab. Eng. Syst. Saf.* **2020**, *200*, 106933. [[CrossRef](#)]

13. Huang, Y.; Chen, L.; Chen, P.; Negenborn, R.R.; van Gelder, P.H.A.J.M. Ship collision avoidance methods: State-of-the-art. *Saf. Sci.* **2020**, *121*, 451–473. [\[CrossRef\]](#)
14. Graziano, A.; Teixeira, A.P.; Guedes Soares, C. Classification of human errors in grounding and collision accidents using the tracer taxonomy. *Saf. Sci.* **2016**, *86*, 245–257. [\[CrossRef\]](#)
15. Sandhåland, H.; Oltedal, H.; Eid, J. Situation awareness in bridge operations—A study of collisions between attendant vessels and offshore facilities in the North Sea. *Saf. Sci.* **2015**, *79*, 277–285. [\[CrossRef\]](#)
16. Fujii, Y.; Shiobara, R. The analysis of traffic accidents. *J. Navig.* **1971**, *24*, 543–552. [\[CrossRef\]](#)
17. Goodwin, E.M. A statistical study of ship domains. *J. Navig.* **1975**, *28*, 328–344. [\[CrossRef\]](#)
18. Coldwell, T.G. Marine traffic behaviour in restricted waters. *J. Navig.* **1983**, *36*, 430–444. [\[CrossRef\]](#)
19. Fiskin, R.; Nasiboglu, E.; Yardimci, M.O. A knowledge-based framework for two-dimensional (2D) asymmetrical polygonal ship domain. *Ocean Eng.* **2020**, *202*, 107187. [\[CrossRef\]](#)
20. Wang, N. A novel analytical framework for dynamic quaternion ship domains. *J. Navig.* **2013**, *66*, 265–281. [\[CrossRef\]](#)
21. Szlapczynski, R.; Szlapczynska, J. Review of ship safety domains: Models and applications. *Ocean Eng.* **2017**, *145*, 277–289. [\[CrossRef\]](#)
22. Baldauf, M.; Mehdi, R.; Fischer, S.; Gluch, M. A perfect warning to avoid collisions at sea? *Sci. J. Mar. Univ. Szczec.* **2017**, *49*, 53–64. [\[CrossRef\]](#)
23. Li, B.; Pang, F. An approach of vessel collision risk assessment based on the D-S evidence theory. *Ocean Eng.* **2013**, *74*, 16–21. [\[CrossRef\]](#)
24. REN, Y.; Mou, J.; Yan, Q.; Zhang, F. Study on assessing dynamic risk of ship collision. In Proceedings of the International Conference on Transportation Information and Safety, Wuhan, China, 2 July 2011; pp. 2751–2757.
25. Li, S.; Liu, J.; Negenborn, R.R. Distributed coordination for collision avoidance of multiple ships considering ship maneuverability. *Ocean Eng.* **2019**, *181*, 212–226. [\[CrossRef\]](#)
26. Simsir, U.; Amasyali, M.F.; Bal, M.; Çelebi, U.B.; Ertugrul, S. Decision support system for collision avoidance of vessels. *Appl. Soft Comput.* **2014**, *25*, 369–378. [\[CrossRef\]](#)
27. Perera, L.P.; Carvalho, J.P.; Guedes Soares, C. Intelligent ocean navigation and fuzzy-bayesian decision/action formulation. *IEEE J. Ocean. Eng.* **2012**, *37*, 204–219. [\[CrossRef\]](#)
28. Cheng, Y.; Zhang, W. Concise deep reinforcement learning obstacle avoidance for underactuated unmanned marine vessels. *Neurocomputing* **2018**, *272*, 63–73. [\[CrossRef\]](#)
29. Perera, L.P.; Guedes Soares, C. Collision risk detection and quantification in ship navigation with integrated bridge systems. *Ocean Eng.* **2015**, *109*, 344–354. [\[CrossRef\]](#)
30. Balmat, J.-F.; Lafont, F.; Maifret, R.; Pessel, N. MARitime risk assessment (MARISA), a fuzzy approach to define an individual ship risk factor. *Ocean Eng.* **2009**, *36*, 1278–1286. [\[CrossRef\]](#)
31. Goerlandt, F.; Montewka, J.; Kuzmin, V.; Kujala, P. A risk-informed ship collision alert system: Framework and application. *Saf. Sci.* **2015**, *77*, 182–204. [\[CrossRef\]](#)
32. Chen, D.; Wan, X.; Dai, C.; Mou, J. A research on AIS-based embedded system for ship collision avoidance. In Proceedings of the 2015 International Conference on Transportation Information and Safety (ICTIS), Wuhan, China, 25–28 June 2015.
33. Xie, S.; Garofano, V.; Chu, X.; Negenborn, R.R. Model predictive ship collision avoidance based on Q-learning beetle swarm antenna search and neural networks. *Ocean Eng.* **2019**, *193*, 106609. [\[CrossRef\]](#)
34. Yoo, Y.; Lee, J.-S. Evaluation of ship collision risk assessments using environmental stress and collision risk models. *Ocean Eng.* **2019**, *191*, 106527. [\[CrossRef\]](#)
35. Liu, Z.; Wu, Z.; Zheng, Z. A cooperative game approach for assessing the collision risk in multi-vessel encountering. *Ocean Eng.* **2019**, *187*, 106175. [\[CrossRef\]](#)
36. Chauvin, C.; Lardjane, S.; Morel, G.; Clostermann, J.-P.; Langard, B. Human and organisational factors in maritime accidents: Analysis of collisions at sea using the HFACS. *Accid. Anal. Prev.* **2013**, *59*, 26–37. [\[CrossRef\]](#)
37. Chen, L.; Liu, C. Improved hierarchical A-star algorithm for optimal parking path planning of the large Parking Lot. In Proceedings of the IEEE International Conference on Information and Automation, Hailar, China, 30 July 2014; pp. 695–698.

38. Wang, H.; Zhou, J.; Zheng, G.; Liang, Y. HAS: Hierarchical a-star algorithm for big map navigation in special areas. In Proceedings of the 5th International Conference on Digital Home (ICDH), Guangzhou, China, 28–30 November 2014; pp. 222–225, ISBN 978-1-4799-4284-8.
39. Xie, L.; Xue, S.; Zhang, J.; Zhang, M.; Tian, W.; Haugen, S. A path planning approach based on multi-direction A* algorithm for ships navigating within wind farm waters. *Ocean Eng.* **2019**, *184*, 311–322. [[CrossRef](#)]
40. Liu, S.; Wang, C.; Zhang, A. A method of path planning on safe depth for unmanned surface vehicles based on hydrodynamic analysis. *Appl. Sci.* **2019**, *9*, 3228. [[CrossRef](#)]
41. Zhang, J.; Zhang, D.; Yan, X.; Haugen, S.; Guedes Soares, C. A distributed anti-collision decision support formulation in multi-ship encounter situations under COLREGs. *Ocean Eng.* **2015**, *105*, 336–348. [[CrossRef](#)]
42. Kim, D.; Hirayama, K.; Okimoto, T. Ship collision avoidance by distributed tabu search. *Int. J. Mar. Navig. Saf. Sea Transp.* **2015**, *9*, 23–29.
43. Kim, D.; Hirayama, K.; Okimoto, T. Distributed stochastic search algorithm for multi-ship encounter situations. *J. Navig.* **2017**, *70*, 699–718. [[CrossRef](#)]
44. Li, S.; Liu, J.; Cao, X.; Zhang, Y. A novel method for solving collision avoidance problem in multiple ships encounter situations. In Proceedings of the 9th International Conference on Computational Linguistics, Vietri sul Mare, Italy, 1–3 October 2018; Volume 11184, pp. 47–66. [[CrossRef](#)]
45. Xie, S.; Chu, X.; Zheng, M.; Liu, C. Ship predictive collision avoidance method based on an improved beetle antennae search algorithm. *Ocean Eng.* **2019**, *192*, 106542. [[CrossRef](#)]
46. Shen, H.; Hashimoto, H.; Matsuda, A.; Taniguchi, Y.; Terada, D.; Guo, C. Automatic collision avoidance of multiple ships based on deep Q-learning. *Appl. Ocean Res.* **2019**, *86*, 268–288. [[CrossRef](#)]
47. Zhao, L.; Roh, M.-I. COLREGs-compliant multiship collision avoidance based on deep reinforcement learning. *Ocean Eng.* **2019**, *191*, 106436. [[CrossRef](#)]
48. Ożoga, B.; Montewka, J. Towards a decision support system for maritime navigation on heavily trafficked basins. *Ocean Eng.* **2018**, *159*, 88–97. [[CrossRef](#)]
49. Xu, Q.; Wang, N. A Survey on Ship Collision Risk Evaluation. *Promet Traffic Transp.* **2014**, *26*, 475–486. [[CrossRef](#)]
50. Yao, J.; Ren, Y.; Wu, Z.; Fang, X. Fuzzy identification method for collision risk assessment of multi-ships encounter situation. *J. Dalian Fish. Univ.* **2002**, *17*, 313–317. [[CrossRef](#)]
51. Wu, B.; Cheng, T.; Yip, T.L.; Wang, Y. Fuzzy logic based dynamic decision-making system for intelligent navigation strategy within inland traffic separation schemes. *Ocean Eng.* **2020**, *197*, 106909. [[CrossRef](#)]
52. Wu, B.; Yip, T.L.; Yan, X.; Guedes Soares, C. Fuzzy logic based approach for ship-bridge collision alert system. *Ocean Eng.* **2019**, *187*, 106152. [[CrossRef](#)]
53. Ahn, J.-H.; Rhee, K.-P.; You, Y.-J. A study on the collision avoidance of a ship using neural networks and fuzzy logic. *Appl. Ocean Res.* **2012**, *37*, 162–173. [[CrossRef](#)]
54. Yan, Q. A model for estimating the risk degrees of collisions. *J. Wuhan Univ. Technol.* **2002**, *26*, 74–76.

